



PAPER

# High-performance photodetector based on semi-encompassed $\text{CH}_3\text{NH}_3\text{PbCl}_3$ -ZnO microwire heterojunction with alterable spectral response

To cite this article: Zhen Cheng *et al* 2023 *Phys. Scr.* **98** 035520

View the [article online](#) for updates and enhancements.

## You may also like

- [Strain effects in a single ZnO microwire with wavy configurations](#)  
Jong Bae Park, Woong-Ki Hong, Tae Sung Bae et al.
- [Room temperature non-balanced electric bridge ethanol gas sensor based on a single ZnO microwire](#)  
Yun-Zheng Li, Qiu-Ju Feng et al.
- [Room-temperature polariton waveguide effect in a ZnO microwire](#)  
Yanjing Ling, Wei Xie, Liaoxin Sun et al.



## PAPER

# High-performance photodetector based on semi-encompassed $\text{CH}_3\text{NH}_3\text{PbCl}_3$ -ZnO microwire heterojunction with alterable spectral response

RECEIVED  
9 November 2022REVISED  
6 February 2023ACCEPTED FOR PUBLICATION  
14 February 2023PUBLISHED  
23 February 2023Zhen Cheng<sup>1</sup>, Kewei Liu<sup>1,2</sup> , Baoshi Qiao<sup>1</sup> , Jialin Yang<sup>1</sup>, Xing Chen<sup>1</sup>, Qiu Ai<sup>1</sup>, Yongxue Zhu<sup>1</sup>, Binghui Li<sup>1</sup> , Lei Liu<sup>1,2</sup> and Dezhen Shen<sup>1,2</sup><sup>1</sup> State Key Laboratory of Luminescence and Applications, Changchun Institute of Optics, Fine Mechanics and Physics, Chinese Academy of Sciences, No.3888 Dongnanhu Road, Changchun, 130033, People's Republic of China<sup>2</sup> Center of Materials Science and Optoelectronics Engineering, University of the Chinese Academy of Sciences, Beijing 100049, People's Republic of ChinaE-mail: [liukw@ciomp.ac.cn](mailto:liukw@ciomp.ac.cn) and [shendz@ciomp.ac.cn](mailto:shendz@ciomp.ac.cn)**Keywords:** perovskite crystallites, ZnO microwires, heterojunction, photodetectorSupplementary material for this article is available [online](#)

## Abstract

Recently, heterojunctions consisting of hybrid organic-inorganic lead (Pb) halide perovskites and other semiconductors have drawn increasing attention for the potential application in photodetectors due to their exceptional performance. However, their performance is usually limited by the relatively low crystalline quality of perovskites, and the response spectra of the devices are difficult to adjust according to the practical requirement. Here, high quality  $\text{CH}_3\text{NH}_3\text{PbCl}_3$  micro-sized crystals have been successfully fabricated on one side of individual ZnO microwire to form heterojunction photodetector by a two-step crystallization method. The heterojunction device presents a low dark current (60 nA at  $-6$  V) along with a rapid response speed (rise time of  $< 20$   $\mu\text{s}$  and fall time of  $\sim 500$   $\mu\text{s}$ ). More interestingly, the modulation of the response spectra and the responsivity can be realized by operating the device under front or back illumination due to the self-filtering properties. Our findings provide a promising method for combining perovskites with other inorganic materials to form high-performance heterojunction photodetectors.

## 1. Introduction

Over recent years, organic-inorganic hybrid perovskite materials,  $\text{CH}_3\text{NH}_3\text{PbX}_3$  ( $X = \text{Cl}^-$ ,  $\text{Br}^-$  and  $\text{I}^-$ ), have grown to be a hit topics in the field of optoelectronic facilities, such as light-emitting diodes, solar cells, lasers and photodetectors [1–12]. In particular, owing to their exceptional optoelectronic characteristics (such as adjustable direct band gap, excellent bipolar charge transport performance, and high light absorption coefficient),  $\text{CH}_3\text{NH}_3\text{PbX}_3$ -based photodetectors have attracted increasing attention, and the devices with various structures have been demonstrated, including metal-semiconductor-metal (MSM), heterojunction and schottky structures [13–17]. Compared with the devices based on pure perovskites, the heterojunction photodetectors composed of perovskites and other semiconductors illustrate more exceptional performance due to the built-in electrical field at the interface of heterojunctions, which could effectively separate the photo-generated carriers [18–21]. For example, an superhigh responsivity of  $\sim 10^9$  A/W have been demonstrated in the perovskite/organic-semiconductor vertical heterojunction photodetectors [22]. Germanium/ $\text{CH}_3\text{NH}_3\text{PbI}_3$  heterojunction showed an outstanding responsivity of  $228 \text{ A W}^{-1}$  at 680 nm due to the photoconductive gain boost [23]. Among the  $\text{CH}_3\text{NH}_3\text{PbX}_3$  perovskites,  $\text{CH}_3\text{NH}_3\text{PbCl}_3$  has the widest bandgap of  $\sim 3.11$  eV, which is considered to be an desired candidate for the fabrication of ultraviolet (UV) photodetectors [24–26]. So far, most reported  $\text{CH}_3\text{NH}_3\text{PbCl}_3$  UV photodetectors are MSM-type devices fabricated on bulk, thin films, and nanostructures [27–30]. Nevertheless, although there are few accounts on heterojunction photodetectors based

on  $\text{CH}_3\text{NH}_3\text{PbCl}_3$  and other semiconductors, significant progress has already been made.  $\text{CH}_3\text{NH}_3\text{PbCl}_3/\text{ZnO}$  hybrid photodetector yielded an exceptional responsivity of  $\sim 1.47 \text{ A W}^{-1}$  and the carriers' separation and transfer amid  $\text{CH}_3\text{NH}_3\text{PbCl}_3$  and ZnO has been demonstrated to be the staple explanation for the performance enhancement [31]. The devices based on polycrystalline  $\text{CH}_3\text{NH}_3\text{PbCl}_3/\text{Ga}_2\text{O}_3$  heterojunctions exhibited excellent self-powered UV photodetection performance and an enhanced UV photoresponsivity can be clearly obtained [32, 33]. However, these reported devices are mainly achieved by spin-coating  $\text{CH}_3\text{NH}_3\text{PbCl}_3$  film onto other semiconductors, and their performance is generally limited by the relatively low crystalline quality of perovskite films [34, 35]. Moreover, the response spectrum of these devices was almost only determined by the individual absorption characteristics of perovskite and semiconductor used for the heterojunction, which cannot be tuned according to the practical requirement.

According to the previous reports, perovskite single crystals generally have low trap-state densities and long carrier diffusion lengths, making them ideal candidates for high-performance optoelectronic applications [36–38]. In this work, the  $\text{CH}_3\text{NH}_3\text{PbCl}_3$  micro-sized crystals have been successfully fabricated on one side of individual ZnO microwire to form heterojunction photodetector by a two-step crystallization method. The x-ray diffraction (XRD) and photoluminescence (PL) results inform that  $\text{CH}_3\text{NH}_3\text{PbCl}_3$  micro-sized crystals preferentially grow along [100] direction perpendicular to the ZnO microwire axial direction and have a high crystalline quality with low defect density. The device has a reduced dark current of 60 nA at  $-6 \text{ V}$  and a rapid rise time and fall time of  $< 20 \mu\text{s}$  and  $\sim 500 \mu\text{s}$ , respectively. More interestingly, the alterable response spectra can be observed under front and back illuminations due to the self-filtering effect. These findings prove that there is tremendous potential in the area of combining perovskite with other inorganic semiconductors to form heterojunction device.

## 2. Experimental section

### 2.1. Preparation of ZnO microwire

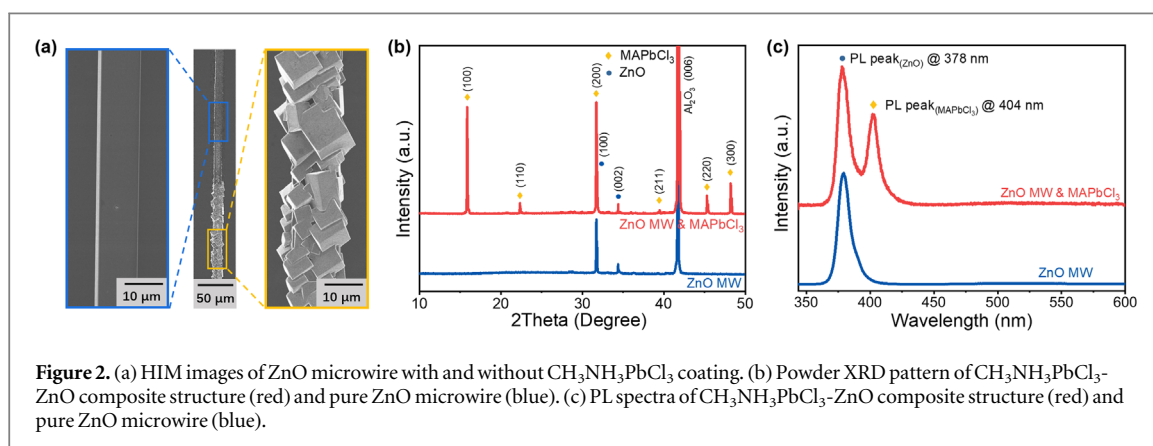
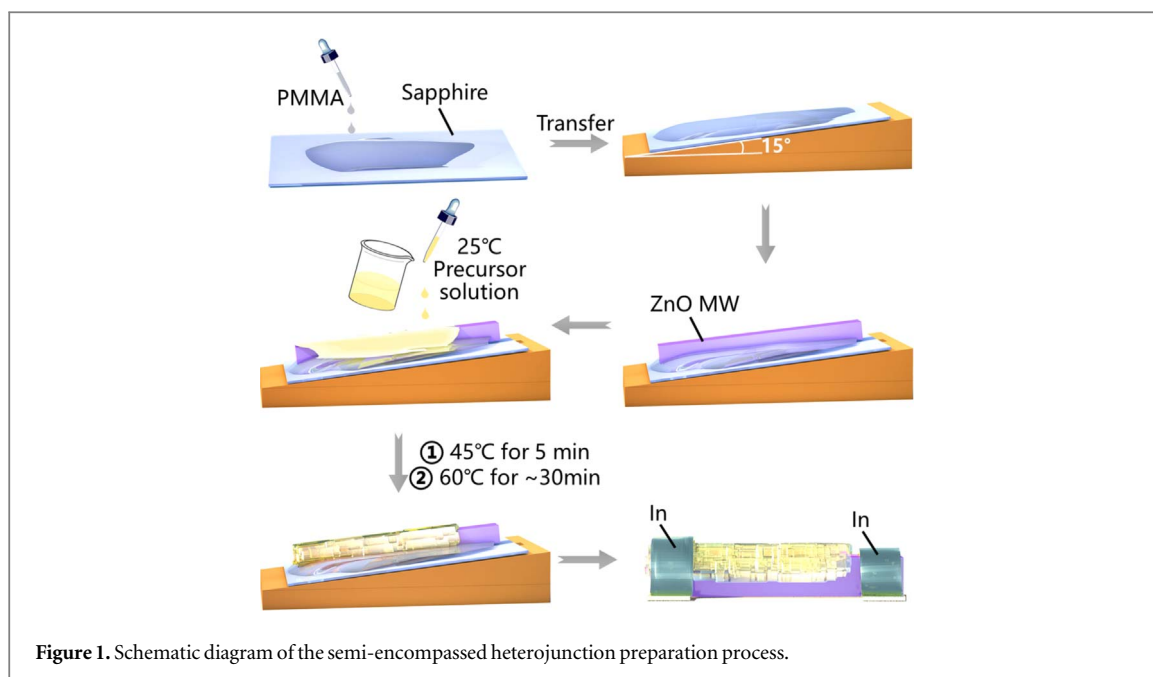
ZnO powder was mixed with the equal weight graphite powder and fully grinded as a source for the preparation of ZnO microwires. The mixture was placed in a corundum boat covered with an ultrasonically cleaned silicon wafer. And then the corundum boat was transferred to the epicenter of the tube furnace. The temperature of tube furnace was raised upto  $1050 \text{ }^\circ\text{C}$  at the rate of  $25 \text{ }^\circ\text{C}$  per minute under argon (99.99%) atmosphere. When the temperature reached  $1050 \text{ }^\circ\text{C}$ , oxygen was inlet into the furnace at a flow rate of  $\sim 15 \text{ sccm}$ , at which point ZnO microwires began to grow. After 45 min, the growth process was finished, and the furnace was cooled down spontaneously. The ZnO microwires obtained by CVD method is shown in figure S1.

### 2.2. Fabrication of the photodetector

Figure 1 shows the schematic preparation process of the semi-encompassed heterojunction based on  $\text{CH}_3\text{NH}_3\text{PbCl}_3\text{-ZnO}$  microwire. An ultrasonically cleaned double-sided polishing sapphire was selected as substrate. Polymethyl methacrylate (PMMA) solution was dripped on the flat sapphire firstly. The substrate was then placed on a plate tilted by 15 degrees, and a ZnO microwire was laid on the substrate with only one side immersed in the PMMA solution. Subsequently, the PMMA solution was naturally dried at room temperature. After that,  $30 \mu\text{l}$  of  $\text{CH}_3\text{NH}_3\text{PbCl}_3$  precursor solution (DMF: DMSO = 1:1) was dropped on the surface of ZnO microwire semi-wrapped of PMMA. Then, the temperature of the hot plate was raised upto  $45 \text{ }^\circ\text{C}$  for 5 min and subsequently raised up to  $60 \text{ }^\circ\text{C}$  until the solvent was completely volatilized. Finally, the flat indium (In) strips were placed on the  $\text{CH}_3\text{NH}_3\text{PbCl}_3$  microcrystalline layer and ZnO microwire, and then carefully pressed them tight to form a semi-encompassed  $\text{CH}_3\text{NH}_3\text{PbCl}_3\text{-ZnO}$  microwire heterojunction photodetector.

### 2.3. Characterization and measurements

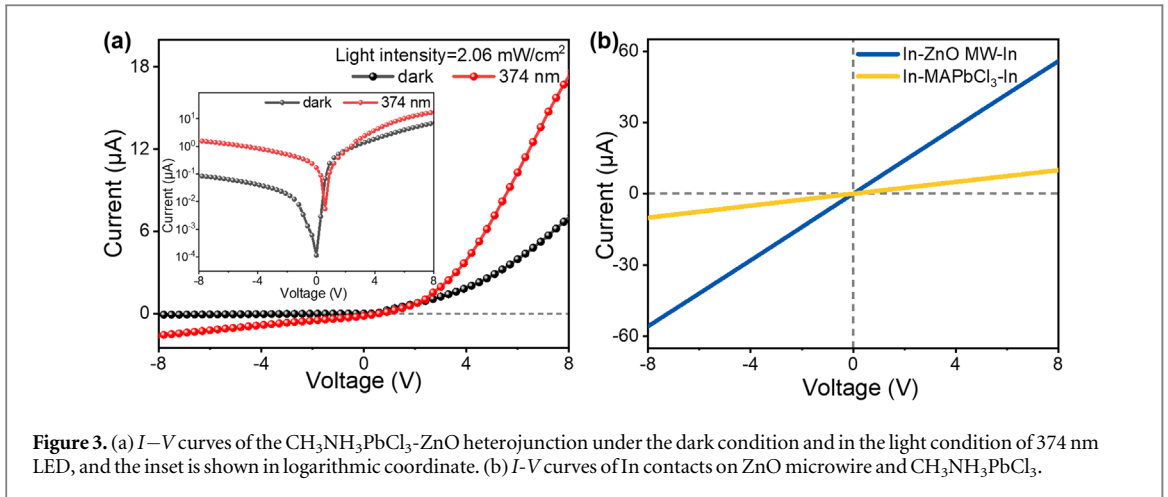
The surface morphology of the  $\text{CH}_3\text{NH}_3\text{PbCl}_3\text{-ZnO}$  composite structure was measured by helium ion microscope (HIM) (Zeiss Orion NanoFab) with accelerating voltage of 30 kV and scanning electron microscope (SEM) (HITACHI S-4800) with accelerating voltage of 5 kV. The PL spectra were measured with a 325 nm He – Cd continuous wave (CW) laser as the luminescent pumping source. The measurements of crystal structures of the composite structure and ZnO microwire were performed by XRD (BRUKER D8 Discover) with Cu-K $\alpha$  radiation ( $\lambda = 1.541 \text{ \AA}$ ). The current–voltage ( $I\text{-}V$ ) characteristics and time-dependent current ( $I\text{-}t$ ) characteristics were tested by a semiconductor parameter analyzer (Keithely 2200) with a 374 nm light-emitting diode. The photoresponse spectra were tested using a 200 W UV-enhanced xenon lamp with a monochromator.



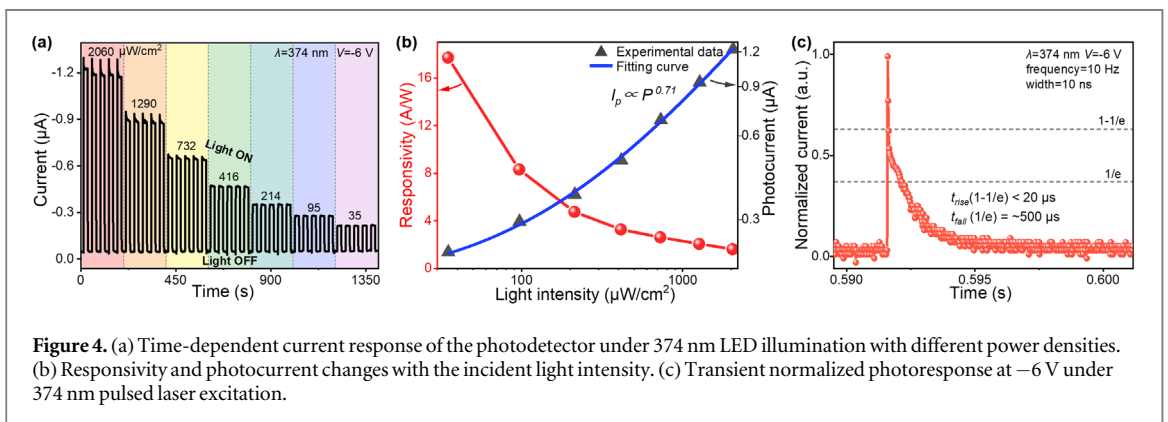
### 3. Results and discussion

Figure 2(a) shows the configurations of the ZnO microwire with and without  $\text{CH}_3\text{NH}_3\text{PbCl}_3$  coating. It can be found the ZnO microwire has a parallelepiped structure with flat and smooth surface. Meanwhile, the covered  $\text{CH}_3\text{NH}_3\text{PbCl}_3$  exhibits a dense layer stacked by cubic micro-crystallites. In addition, the diameter of ZnO microwire is around  $10\ \mu\text{m}$  and the average thickness of the  $\text{CH}_3\text{NH}_3\text{PbCl}_3$  layer is about  $3\ \mu\text{m}$ .

To further investigate the crystallographic structure of the  $\text{CH}_3\text{NH}_3\text{PbCl}_3$  microcrystals and ZnO microwire, XRD measurement in the  $2\theta$  scan mode was performed as shown in figure 2(b). For bare ZnO microwire, a strong diffraction peak at  $31.7^\circ$  and a weak diffraction peak at  $34.4^\circ$  may be distributed to (100) and (002) crystallographic planes of the wurtzite ZnO crystal structure (JCPDS No. 36-1451). After coating with  $\text{CH}_3\text{NH}_3\text{PbCl}_3$  crystallites, new sharp peaks appear at  $15.8^\circ$ ,  $22.3^\circ$ ,  $31.7^\circ$ ,  $39.3^\circ$ ,  $45.2^\circ$  and  $48.1^\circ$ , corresponding to (100), (110), (200), (211), (220) and (300) lattice planes of the cubic  $\text{CH}_3\text{NH}_3\text{PbCl}_3$  crystal structure, respectively. The strong (100), (200) and even (300) diffraction peaks indicate that  $\text{CH}_3\text{NH}_3\text{PbCl}_3$  micro-sized crystals preferentially grow along [100] direction perpendicular to the ZnO microwire axial direction, which is in corcking accord with the HIM images. The narrow full width at half maximum (FWHM) for the (100) diffraction peak of  $\text{CH}_3\text{NH}_3\text{PbCl}_3$  is only  $0.09^\circ$ , which is very close to the results of  $\text{CH}_3\text{NH}_3\text{PbCl}_3$  single crystals, illustrating the excellent crystalline quality [28]. And there are no additional peaks from impurities in the spectra. Figure 2(c) reveals the PL spectra of  $\text{CH}_3\text{NH}_3\text{PbCl}_3$ -ZnO hybrid structure and bare ZnO microwire at room temperature. The photoluminescence peak located at  $378\ \text{nm}$  with the FWHM of  $10.41\ \text{nm}$  corresponds to the near-band-edge (NBE) emission of ZnO microwire. Almost no visible emission related to the defects luminescence can be observed, suggesting the splendid crystalline quality of ZnO microwire. Compared with bare ZnO microwire, the PL spectrum of  $\text{CH}_3\text{NH}_3\text{PbCl}_3$ -ZnO hybrid structure shows a new peak at  $404\ \text{nm}$



**Figure 3.** (a)  $I$ - $V$  curves of the  $\text{CH}_3\text{NH}_3\text{PbCl}_3$ -ZnO heterojunction under the dark condition and in the light condition of 374 nm LED, and the inset is shown in logarithmic coordinate. (b)  $I$ - $V$  curves of In contacts on ZnO microwire and  $\text{CH}_3\text{NH}_3\text{PbCl}_3$ .



**Figure 4.** (a) Time-dependent current response of the photodetector under 374 nm LED illumination with different power densities. (b) Responsivity and photocurrent changes with the incident light intensity. (c) Transient normalized photoresponse at  $-6$  V under 374 nm pulsed laser excitation.

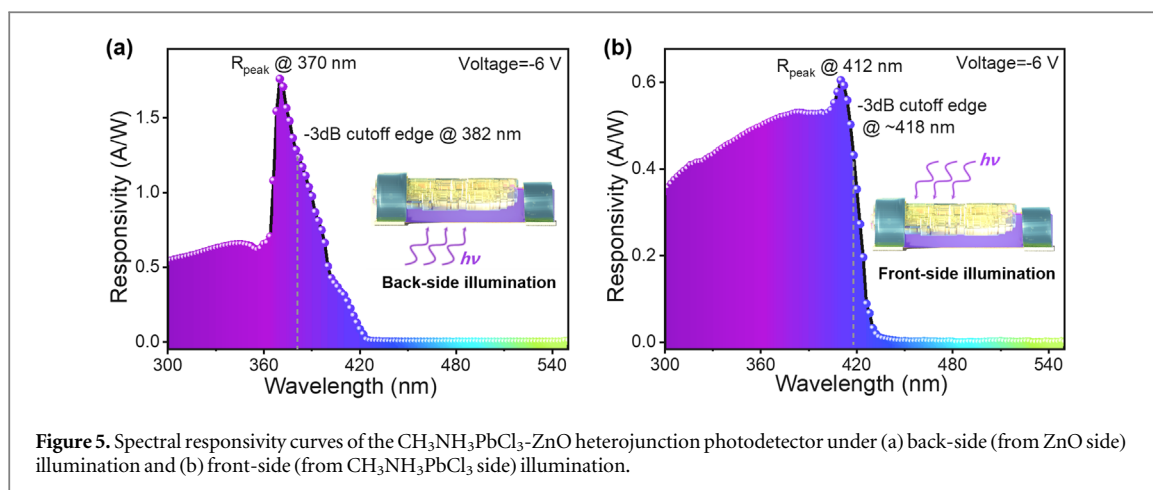
with FWHM of 11.72 nm, originating from the NBE emission of  $\text{CH}_3\text{NH}_3\text{PbCl}_3$  crystallites. The strong and narrow NBE emission peaks and the absence of defect-related visible emission indicate that both ZnO and  $\text{CH}_3\text{NH}_3\text{PbCl}_3$  have high crystalline quality.

Figure 3(a) displays the  $I$ - $V$  characteristics of the  $\text{CH}_3\text{NH}_3\text{PbCl}_3$ -ZnO heterojunction photodetector in the dark condition and under 374 nm illumination ( $2.06 \text{ mW cm}^{-2}$ ) from ZnO side plotted in both linear and logarithmic coordinates (inset). The heterojunction device shows obvious rectification characteristic with a rectifier ratio of 67 at the bias of  $\pm 6$  V under dark condition. At  $-6$  V, the dark current of the photodetector is  $\sim 60$  nA. Figure 3(b) gives the  $I$ - $V$  characteristics of the In/ZnO and In/ $\text{CH}_3\text{NH}_3\text{PbCl}_3$  contacts. It can be seen the two curves are almost linear, indicating that In electrodes on both  $\text{CH}_3\text{NH}_3\text{PbCl}_3$  and ZnO are ohmic contacts. This phenomenon shows that the rectifying behavior comes from the  $\text{CH}_3\text{NH}_3\text{PbCl}_3$ -ZnO heterojunction rather than the metal-semiconductor contacts.

Figure 4(a) depicts the time-dependent current response of the heterojunction device under 374 nm illumination from ZnO side with the power densities differing from 3270 to  $15 \mu\text{W/cm}^2$ . After multiple ON/OFF switching cycles, the device still shows a stable optical response and fast response speed, suggesting the exceptional stability and reproducibility. In addition, the photocurrent overshooting phenomenon can be clearly observed under high-power intensity light illumination due to the instantaneous generation of vast excess carriers [39]. Then, with the decrease of the light intensity, the overshooting phenomenon gradually weakens until it disappears. The responsivity ( $R$ ) of this photodetector at different light intensities could be determined by the pursuing formula:

$$R = \frac{I_{\text{light}} - I_{\text{dark}}}{P_{\text{light}} \cdot S} \quad (1)$$

Where  $I_{\text{light}}$  is the current under light irradiation,  $I_{\text{dark}}$  is the dark current,  $P_{\text{light}}$  is the incident optical power density and  $S$  is the effective absorptive area. The changes of photocurrent and responsivity along with power intensity are given in figure 4(b). It could be noticed that the relation between photocurrent and incident light intensity can be described by the power function of  $I_p \propto P^\theta$ , and  $\theta$  is estimated to be  $\sim 0.71$ , indicating the existence of defects within the device [40].



Considering the high crystalline quality of both ZnO and  $\text{CH}_3\text{NH}_3\text{PbCl}_3$ , the defects should mainly exist at the  $\text{CH}_3\text{NH}_3\text{PbCl}_3\text{-ZnO}$  interface. In addition, the responsivity gradually decreases as the light intensity increasing due to the increased recombination loss of photo-generated carriers under strong light [41–43]. And the responsivity of the device reaches up to  $17.69 \text{ A/W}$  under illumination intensity of  $35 \mu\text{W}/\text{cm}^2$ .

To further appraise the response time of this  $\text{CH}_3\text{NH}_3\text{PbCl}_3\text{-ZnO}$  heterojunction photodetector, a 374 nm Nd:YAG pulsed laser (spot size diameter:  $\sim 1.5 \text{ mm}$ ; frequency: 10 Hz; width: 10 ns) and an oscilloscope are selected to measure the photoresponse signal, and the transient photoresponse curves are shown in figure 4(c). It is conspicuous that the heterojunction photodetector has a fleet response speed, with the rise time ( $t_{\text{rise}}$ , from the dark current to  $(1-1/e)$  of the peak value) of  $< 20 \mu\text{s}$  and fall time ( $t_{\text{fall}}$ , recovery to  $1/e$  of the peak value) of  $\sim 500 \mu\text{s}$  [44].

The spectral response characteristics of this photodetector are measured under contrary illumination directions. The photoresponse curve of the device illuminated from the ZnO microwire side (back side) is shown in figure 5(a). It can be found that a distinct peak value position is located at 370 nm accompanied by the  $-3\text{dB}$  cutoff edge of 382 nm, and the full width at half-maximum (FWHM) of the response peak value is approximately 30 nm. In contrast, under the illumination from  $\text{CH}_3\text{NH}_3\text{PbCl}_3$  side (front side), the response peak position shifts to 412 nm and the  $-3 \text{ dB}$  cutoff wavelength is located at 418 nm (figure 5(b)). Moreover, the peak responsivities of the  $\text{CH}_3\text{NH}_3\text{PbCl}_3\text{-ZnO}$  heterojunction photodetector under back-side illumination and front-side illumination are  $1.6$  and  $0.6 \text{ A W}^{-1}$ , respectively. The modulation of the response spectra and the responsivity by operating the device under front or back illumination can be explained by self-filtering properties.

As the energy bandgap of  $\text{CH}_3\text{NH}_3\text{PbCl}_3$  (3.1 eV) is narrower than that of ZnO (3.37 eV), when the device operates under front-side illumination, the incident photons below 410 nm are mainly absorbed by the  $\text{CH}_3\text{NH}_3\text{PbCl}_3$  layer, making the response spectrum similar to that of pure  $\text{CH}_3\text{NH}_3\text{PbCl}_3$  device [45]. Nevertheless, when the device is irradiated from backside, ZnO microwire is not only the sensing layer, but also acts as a filter layer, consequently, the device exhibits a strong response to the photons in the wavelength regime of 360 nm to 400 nm. Due to the strong NEB absorption of both ZnO and  $\text{CH}_3\text{NH}_3\text{PbCl}_3$ , the responsivity of  $\text{CH}_3\text{NH}_3\text{PbCl}_3\text{-ZnO}$  heterojunction under back-side illumination is obviously higher than that under front-side illumination.

## 4. Conclusions

In this work, we fabricate high-quality  $\text{CH}_3\text{NH}_3\text{PbCl}_3$  micro-crystals on one side of individual ZnO microwire to build a semi-encompassed  $\text{CH}_3\text{NH}_3\text{PbCl}_3\text{-ZnO}$  heterojunction photodetector by a two-step crystallization method. The dark current of the photodetector is solely 60 nA at  $-6 \text{ V}$ , which is significantly lower than that of sole  $\text{CH}_3\text{NH}_3\text{PbCl}_3$  or ZnO devices. In addition, the rise time and fall time are  $< 20 \mu\text{s}$  and  $\sim 500 \mu\text{s}$ , respectively, indicating that the device has a fleet response speed. Interestingly, the device can also obtain an alterable spectral photoresponse by changing the illumination direction. Our troves in this piece afford a viable means of realizing high-performance optoelectronic facilities based on heterojunctions of perovskite and other semiconductor materials.



## Acknowledgments

This work was supported by the National Natural Science Foundation of China (Nos. 62074148, 61875194, 12204474, and 11727902), the National Ten Thousand Talent Program for Young Top-notch Talents, the 100 Talents Program of the Chinese Academy of Sciences, the Key Research and Development Program of Changchun City (No. 21ZY05), Youth Innovation Promotion Association, CAS (No. 2020225), Jilin Province Science Fund (20220101053JC, and 20210101145JC), XuGuang Talents Plan of CIOMP.

## Data availability statement

All data that support the findings of this study are included within the article (and any supplementary files).


## Supporting Information

Photograph of ZnO microwires prepared by CVD method; SEM image of ZnO microwire partially immersed in PMMA; EDS line scanning curves of element distribution of Zn and Pb in the  $\text{CH}_3\text{NH}_3\text{PbCl}_3$ -ZnO composite structure.

## Conflicts of interest

The authors affirm no conflict of financial/commercial interest.

## ORCID iDs

Kewei Liu  <https://orcid.org/0000-0001-5086-0410>  
Baoshi Qiao  <https://orcid.org/0000-0002-5095-1344>  
Binghui Li  <https://orcid.org/0000-0002-6704-2809>  
Lei Liu  <https://orcid.org/0000-0002-9714-2130>

## References

- [1] Liu Y, Yang Z and Liu S F 2018 *Adv. Sci.* **5** 1700471
- [2] Rana N and Samanta P 2022 *Phys. Scr.* **97** 115816
- [3] Ke L, Luo S, Ren X and Yuan Y 2021 *J. Phys. D: Appl. Phys.* **54** 163001
- [4] Chen J, Zhou Y, Fu Y, Pan J, Mohammed O F and Bakr O M 2021 *Chem. Rev.* **121** 12112–80
- [5] Ejaz A, Mustafa G, Amin M, Noor N, Ullah H and Neffati R 2022 *Phys. Scr.* **97** 115704
- [6] Jena A K, Kulkarni A and Miyasaka T 2019 *Chem. Rev.* **119** 3036–103
- [7] Liu H, Zhang X, Zhang L, Yin Z, Wang D, Meng J, Jiang Q, Wang Y and You J 2017 *J. Mater. Chem. C* **5** 6115–22
- [8] Ghosh J, Ghosh R and Giri P K 2019 *ACS Appl. Mater. Inter.* **11** 14917–31
- [9] Tang J, Sie Y, Tseng Z, Lin J, Chen L and Hsu C 2022 *ACS Appl. Nano Mater.* **5** 7237–45
- [10] Ghosh J, Mawlong L P L, G. B M, Pattison A J, Theis W, Chakraborty S and Giri P K 2020 *J. Mater. Chem. C* **8** 8917–34
- [11] Ghosh J and Giri P K 2021 *J. Phys. Mater.* **4** 032008
- [12] Ghosh J, Natu G and Giri P K 2019 *Org. Electron.* **71** 175–84
- [13] Li L, Ye S, Qu J, Zhou F, Song J and Shen G 2021 *Small* **17** e2005606
- [14] Mei F, Sun D, Mei S, Feng J, Zhou Y, Xu J and Xiao X 2019 *Adv. Phys. X* **4** 1592709
- [15] Wang F et al 2021 *Adv. Sci.* **8** e2100569
- [16] Jing H et al 2020 *Nano Lett.* **20** 7144–51
- [17] Zhang M, Lu Q, Wang C, Dai H, Xue Y, He J and Ge B 2020 *J. Phys. D: Appl. Phys.* **53** 235107
- [18] Xie C, Liu C K, Loi H L and Yan F 2019 *Adv. Func. Mater.* **30** 1903907
- [19] Chen F, Shi Z, Chen J, Cui Q, Jian A, Zhu Y, Xu Q, Lou Z and Xu C 2021 *Appl. Phys. Lett.* **118** 171901
- [20] Shen Y, Wei C, Ma L, Wang S, Wang X, Xu X and Zeng H 2018 *J. Mater. Chem. C* **6** 12164–9
- [21] Wu C Y, Peng W, Fang T, Wang B, Xie C, Wang L, Yang W H and Luo L B 2019 *Adv. Electron. Mater.* **5** 1900135
- [22] Xie C, You P, Liu Z, Li L and Yan F 2017 *Light: Sci. Appl.* **6** e17023
- [23] Hu W, Cong H, Huang W, Huang Y, Chen L, Pan A and Xue C 2019 *Light: Sci. Appl.* **8** 106
- [24] Adinolfi V, Ouellette O, Saidaminov M I, Walters G, Abdelhady A L, Bakr O M and Sargent E H 2016 *Adv. Mater.* **28** 7264–8
- [25] Nandi P, Giri C, Swain D, Manju U and Topwal D 2019 *Cryst. Eng. Comm.* **21** 656–61
- [26] Yuan Z, Huang W, Ma S, Ouyang G, Hu W and Zhang W 2019 *J. Mater. Chem. C* **7** 5442–50
- [27] Ding J, Cheng X, Jing L, Zhou T, Zhao Y and Du S 2018 *ACS Appl. Mater. Inter.* **10** 845–50
- [28] Cheng X, Jing L, Zhao Y, Du S, Ding J and Zhou T 2018 *J. Mater. Chem. C* **6** 1579–86
- [29] Maculan G, Sheikh A D, Abdelhady A L, Saidaminov M I, Haque M A, Murali B, Alarousu E, Mohammed O F, Wu T and Bakr O M 2015 *J. Phys. Chem. Lett.* **6** 3781–6
- [30] Wang W et al 2016 *Opt. Express* **24** 8411–9
- [31] Yang J et al 2018 *ACS Appl. Mater. Inter.* **10** 34744–50

- [32] Liu S, Jiao S, Lu H, Nie Y, Gao S, Wang D, Wang J and Zhao L 2022 *J. Alloy. Compd.* **890** 161827
- [33] Liu S, Jiao S, Zhang J, Lu H, Wang D, Gao S, Wang J and Zhao L 2022 *Appl. Surf. Sci.* **571** 151291
- [34] Edri E, Kirmayer S, Henning A, Mukhopadhyay S, Gartsman K, Rosenwaks Y, Hodes G and Cahen D 2014 *Nano Lett.* **14** 1000–4
- [35] Cho N et al 2016 *Nat. Commun.* **7** 13407
- [36] Dong Q, Fang Y, Shao Y, Mulligan P, Qiu J, Cao L and Huang J J S 2015 *Sci.* **347** 967–70
- [37] Feng A, Jiang X, Zhang X, Zheng X, Zheng W, Mohammed O F, Chen Z and Bakr O M 2020 *Chem. Mater.* **32** 7602–17
- [38] Arya S, Mahajan P, Gupta R, Srivastava R, Tailor N K, Satapathi S, Sumathi R R, Datt R and Gupta V 2020 *Prog. Solid State Chem.* **60** 100286
- [39] Liu P et al 2012 *J. Appl. Phys.* **112** 083103
- [40] Liu Y et al 2018 *Adv. Mater.* **30** e1707314
- [41] Jiang Y, Zhang W J, Jie J S, Meng X M, Fan X and Lee S T 2007 *Adv. Funct. Mater.* **17** 1795–800
- [42] Li S et al 2019 *ACS Appl. Mater. Inter.* **11** 35105–14
- [43] Kind H, Yan H, Messer B, Law M and Yang P 2002 *Adv. Mater.* **14** 158
- [44] Li C, Wang H, Wang F, Li T, Xu M, Wang H, Wang Z, Zhan X, Hu W and Shen L 2020 *Light: Sci. Appl.* **9** 31
- [45] Cheng Z, Liu K, Yang J, Chen X, Xie X, Li B, Zhang Z, Liu L, Shan C and Shen D 2019 *ACS Appl. Mater. Inter.* **11** 34144–50